Presynaptic inhibition differentially shapes transmission in distinct circuits in the mouse retina

Erika D. Eggers[1], Maureen A. McCall[2,3] and Peter D. Lukasiewicz[1]

[1]*Department of Ophthalmology and Visual Sciences and Anatomy and Neurobiology, Washington University, St Louis MO 63110, USA*
[2]*Department of Psychological and Brain Sciences, and* [3]*Department of Ophthalmology and Visual Sciences, University of Louisville, Louisville, KY 40292, USA*

Diverse retinal outputs are mediated by ganglion cells that receive excitatory input from distinct classes of bipolar cells (BCs). These classes of BCs separate visual signals into rod, ON and OFF cone pathways. Although BC signalling is a major determinant of the ganglion cell-mediated retinal output, it is not fully understood how light-evoked, presynaptic inhibition from amacrine cell inputs shapes BC outputs. To determine whether differences in presynaptic inhibition uniquely modulate BC synaptic output to specific ganglion cells, we assessed the inhibitory contributions of $GABA_A$, $GABA_C$ and glycine receptors across the BC pathways. Here we show that different proportions of $GABA_A$ and $GABA_C$ receptor-mediated inhibition determined the kinetics of GABAergic presynaptic inhibition across different BC classes. Large, slow $GABA_C$ and small, fast $GABA_A$ receptor-mediated inputs to rod BCs prolonged light-evoked inhibitory postsynaptic currents (L-IPSCs), while smaller $GABA_C$ and larger $GABA_A$ receptor-mediated contributions produced briefer L-IPSCs in ON and OFF cone BCs. Glycinergic inhibition also varied across BC class. In the rod-dominant conditions studied here, slow glycinergic inputs dominated L-IPSCs in OFF cone BCs, attributable to inputs from the rod pathway via AII amacrine cells, while rod and ON cone BCs received little and no glycinergic input, respectively. As these large glycinergic inputs come from rod signalling pathways, in cone-dominant conditions L-IPSCs in OFF cone bipolar cells will probably be dominated by $GABA_A$ receptor-mediated input. Thus, unique presynaptic receptor combinations mediate distinct forms of inhibition to selectively modulate BC outputs, enhancing the distinctions among parallel retinal signals.

(Resubmitted 6 March 2007; accepted after revision 23 April 2007; first published online 26 April 2007)
Corresponding author P. D. Lukasiewicz: Department of Ophthalmology, Campus Box 8096, Washington University School of Medicine, 660 S. Euclid Avenue, St Louis, MO 63110, USA. Email: lukasiewicz@vision.wustl.edu

The timecourse of synaptic signalling is governed by the properties of presynaptic neurotransmitter release and the kinetics and complement of postsynaptic receptors. Previous studies in spinal cord and hippocampus have shown that a balance between the timecourse of inhibition and excitation creates maximal inhibitory modulation of the excitatory signal (Hajos & Mody, 1997; Chadderton *et al.* 2004; Takahashi, 2005). In the retina, the excitatory synapse between bipolar cells (BCs) and ganglion cells is a critical determinant of the nature of the retinal output. Since BCs receive significant presynaptic inhibitory input onto their axon terminals, this synapse is ideal for exploring how excitation and presynaptic inhibition interact to shape sensory signals.

Mammalian BCs are divided into three major classes at the first synapse in the retina. Cone photoreceptors contact both ON and OFF BCs that respond to increments and decrements of light intensity, respectively. Rod photoreceptors contact rod BCs that respond to light increments. While the excitatory inputs to these parallel rod and cone BC pathways in the outer retina are temporally distinct, attributable to both distinct presynaptic neurotransmitter release and postsynaptic glutamate receptor types (Ashmore & Copenhagen, 1980; Schnapf & Copenhagen, 1982; Cadetti *et al.* 2005; Li & DeVries, 2006), it is unclear how presynaptic inhibition of BCs in the inner retina shapes their visual output.

BC outputs are shaped by presynaptic inhibitory input from GABAergic and glycinergic amacrine cells (Lukasiewicz & Werblin, 1994; Pan & Lipton, 1995; Dong & Werblin, 1998; Euler & Masland, 2000) onto functionally distinct $GABA_A$, $GABA_C$ and glycine receptors on their axon terminals (Euler & Wassle, 1998; Shields *et al.* 2000; Eggers & Lukasiewicz, 2006*a*). Agonist application studies suggest that the contributions of $GABA_A$, $GABA_C$ and glycine receptors vary with BC class (Euler & Wassle, 1998; Shields *et al.* 2000; Ivanova *et al.* 2006), predicting the distinct shaping of their outputs. However,

 DOI: 10.1113/jphysiol.2007.131763

light-evoked inhibition is influenced both by differences in neurotransmitter release and receptor distribution, and little was known about how this differential contribution by inhibitory receptors affected light-evoked inhibition to bipolar cells. We previously showed that distinct receptors differentially shape the peak amplitude (glycine, $GABA_A$) and timecourse ($GABA_C$) of rod BC output (Eggers & Lukasiewicz, 2006*b*), suggesting that diverse contributions from receptor types could uniquely shape outputs from different BC classes. Additionally, our earlier work suggested that differences in presynaptic inhibition across BC classes shape the visually driven BC outputs to their target ganglion cells (Sagdullaev *et al.* 2006). However, the synaptic mechanisms responsible for these differences remain unknown because light-evoked inhibition to BCs had not been studied.

Here we characterized how different complements of GABAergic and glycinergic inhibitory receptors produce distinct light-evoked inhibition across BC classes. We found that inhibition within a distinct BC class was determined by unique combinations of $GABA_C$, $GABA_A$ and glycine receptors. The timecourse of inhibition across BC classes was well matched to the timecourse of their excitatory inputs that is reported in the literature (Ashmore & Copenhagen, 1980; Schnapf & Copenhagen, 1982; Cadetti *et al.* 2005; Li & DeVries, 2006). Specifically, large slow $GABA_C$ receptor-mediated inputs dominate rod BC light-evoked inhibitory postsynaptic currents (L-IPSCs). Smaller $GABA_C$ receptor-mediated inputs combine with fast $GABA_A$ receptor-mediated inputs to create shorter decays in ON cone BCs. Glycinergic inhibition dominates the response of OFF cone BCs under dark-adapted conditions, but this inhibition is likely to switch to $GABA_A$ receptor-dominated inputs when signalling arises from cone photoreceptor input. Thus, our results suggest that the output of BCs, a major determinant of the retinal output, is shaped by distinct forms of inhibition, adding another level of specificity to visual processing.

Methods

Preparation of mouse retinal slices

Animal protocols were approved by the Washington University School of Medicine Animal Studies Committee. The experimental techniques were similar to those previously described (Eggers & Lukasiewicz, 2006*a*). Briefly, both wild-type (WT) mice (C57BL/6J strain; Jackson Laboratories; Bar Harbour, ME, USA) and $GABA_C$ ρ1 null mice that lacked functional $GABA_C$ receptors in the retina (congenic on a C57BL/6J background) (McCall *et al.* 2002) were used. For brevity we will refer to the knockout mice as $GABA_C$R null, as we have in previous publications (Eggers & Lukasiewicz, 2006*a*,*b*). Mice 28–90 days of age were killed using carbon dioxide, their eyes enucleated and the cornea, lens and vitreous removed. The eyecup was incubated for 20 min in dissection and storage solution (see Electrode and bath solutions) with 0.5 mg ml^{-1} hyaluronidase (Sigma, St Louis, MO, USA). The hyaluronidase solution was replaced with cold, oxygenated storage solution, the retina was dissected out of the eyecup, and 200–250 μm slices were prepared from the isolated retina and maintained in oxygenated storage solution at room temperature.

Whole-cell recordings

Whole-cell patch recordings were made from BCs from retinal slices, as previously described (Eggers & Lukasiewicz, 2006*a*), using recording procedures and apparatus that also have been previously described (Lukasiewicz & Roeder, 1995). IPSCs were recorded from retinal BCs voltage clamped to 0 mV, the reversal potential for currents mediated by non-selective cation channels. Liquid junction potentials of 15 mV were corrected at the beginning of each recording. Electrodes were pulled from borosilicate glass (1B150F-4; World Precision Instruments, Sarasota, FL, USA) on a P97 Flaming/Brown puller (Sutter Instruments, Novato, CA, USA) and had resistances of < 5 MΩ. Patchit software (White Perch Software, Somerville, MA, USA) was used to generate voltage command outputs, acquire data and gate the drug perfusion valves. The data were digitized and stored on a personal computer using a Labmaster DMA data acquisition board (Scientific Solutions, Solon, OH, USA).

Solutions and drugs

The control solution used for dissection, storage and the extracellular recording solution for GABA-evoked responses contained (mM): 137 NaCl, 2.5 KCl, 1 $MgCl_2$, 2.5 $CaCl_2$, 28 glucose and 10 Hepes, was adjusted to pH 7.4 with NaOH and bubbled with O_2. The extracellular recording solution used to examine spontaneous and light-evoked currents contained (mM): 125 NaCl, 2.5 KCl, 1 $MgCl_2$, 1.25 NaH_2PO_4, 2 $CaCl_2$, 20 glucose and 26 $NaHCO_3$ and was bubbled with 95% O_2–5% CO_2. The intracellular solution contained (mM): 120 caesium gluconate, 1 $CaCl_2$, 1 $MgCl_2$, 10 Na-Hepes, 11 EGTA, 10 TEA-Cl and was adjusted to pH 7.2 with CsOH. Antagonists were applied to the slice chamber using a gravity-driven superfusion system. Unless otherwise indicated, all chemicals were obtained from Sigma.

Morphological identification of retinal cell classes

BCs were labelled with either Lucifer yellow (0.05%) or Sulforhodamine B (0.005%), dissolved in the intracellular solution. They were classified as either rod, ON cone

or OFF cone BCs, based on their dendritic and axonal morphologies, and the stratification of their somas in the inner nuclear layer and their axon terminals within the ON and OFF sublaminae of the inner plexiform layer (Ghosh *et al.* 2004).

Light-evoked IPSC recordings

The methods to record light-evoked inhibitory post synaptic currents (L-IPSCs) have been previously described (Eggers & Lukasiewicz, 2006*a*). Mice were dark-adapted overnight and all dissection and recording procedures were performed under infrared illumination to preserve the light sensitivity of the preparations. Recordings were made in extracellular solution heated to 32°C, using thin stage and inline heaters (Cell Micro-controls, Norfolk, VA, USA). Light-evoked responses were filtered at 1 kHz with the four-pole Bessel filter on the Axopatch 200B (Axon Instruments, Foster City, CA, USA) and sampled at 2 kHz. To isolate inhibitory receptor inputs, strychnine (500 nM) was used to block glycine receptors, bicuculline methobromide (50 μM) to block $GABA_A$ receptors and (1,2,5,6-tetrahydropyridine-4yl) methyphosphinic acid (TPMPA, 50 μM) to block $GABA_C$ receptors. L-IPSCs were evoked with a full-field flash using a light-emitting diode (LED, Agilent HLMP-3950, $\lambda_{peak} = 565$ nm, Palo Alto, CA, USA) positioned near the microscope stage. Stimulus intensity (1.85×10^3 photons μm^{-2} s^{-1}) and duration were controlled by current applied to the LED.

GABA-evoked current recordings

Once a whole-cell recording was established, the Lucifer yellow- or sulforhodamine-filled BC axon terminal was briefly visualized and a glass electrode containing 30 μM GABA, dissolved in the control recording solution, was positioned near the axon terminal. GABA currents were evoked by puffing GABA (5–15 lbf in^{-2}) onto the BC axon terminal using a Picospritzer II (General Valve). Recordings of GABA-evoked currents were made at room temperature and were recorded at 500 Hz. For GABA-evoked recordings, the control recording solution contained strychnine (10 μM), CNQX (10 μM) and D-AP5 (50 μM) to eliminate synaptic influences. Bicuculline (500 μM) and TPMPA (50 μM) were used to block $GABA_A$ and $GABA_C$ receptors, respectively.

Spontaneous IPSC recordings

Recordings of spontaneous currents were made in extracellular solution heated to 32°C, in the absence of light stimuli, and were filtered at 1 kHz and sampled at 2–5 kHz. Strychnine (500 nM), bicuculline (50 μM) and TPMPA (50 μM) were used to isolate receptor types, similar to the light-evoked recordings. Kainate (10 μM), which activates AMPA/kainate receptors on amacrine cells, was used to depolarize amacrine cells and increase spontaneous GABA release which enabled the recording of spontaneous $GABA_C$ receptor-mediated currents (Frech & Backus, 2004; Eggers & Lukasiewicz, 2006*b*).

Data analysis and statistics

Tack (White Perch Software, Somerville, MA, USA) and Clampfit (Axon Instruments) software were used to create average response records and to measure the peak, time to peak (from the onset of the light stimulus), charge transfer (Q, pA ms or fC) and decay time (D_{37}, defined below) of L-IPSCs and the Q and decay time of GABA-evoked responses. All light-evoked IPSCs and GABA-evoked responses shown and used in our analyses are an average of two responses from the same cell. Since the decay time could not be easily fitted with either a single or double exponential curve, we determined the decay time by computing the time at which the L-IPSC declined to 37% of its peak amplitude (D_{37}). Student's t tests (two-tailed, unequal variance) were used to compare response characteristics from WT and $GABA_C$R null BCs. An ANOVA with a Scheffé's *post hoc* test was used to compare differences among currents from rod, ON cone and OFF cone BCs. Differences were considered significant when $P \leq 0.05$. All average data are reported as mean ± standard error of the mean (S.E.M.), and n refers to number of cells; N refers to number of sIPSCs. Ratios of averages are reported as ratio ± propagated S.E.M. Propagated errors are defined as:

$$\frac{\text{Ratio}_{\text{error}}}{\text{Ratio}} = \sqrt{\left(\frac{X_{\text{error}}}{X}\right)^2 + \left(\frac{Y_{\text{error}}}{Y}\right)^2}$$

where Ratio = X/Y

Spontaneous IPSCs (sIPSCs) were selected so that the rise and decay phases did not contain any overlapping events, and Mini Analysis software (Synaptosoft, Decatur, GA, USA) was used to measure the amplitude and calculate the τ_{decay}, the time constant of an exponential function fit to the decay from the peak to baseline, of each individual sIPSC. The distributions of sIPSC amplitude and τ_{decay} were compared using the Kolmogorov–Smirnov test (K–S). To compute the average sIPSC, events were aligned at 50% of their rise time and sIPSCs were averaged using Clampfit. As rise time of $GABA_C$ receptor-mediated sIPSCs was too slow to be effectively aligned using the MiniAnalysis program, they were aligned by hand using Clampfit.

Results

GABAergic L-IPSCs show distinct timing across BC classes

Previous work characterizing currents evoked by GABA applications suggests a differential distribution of $GABA_A$ and $GABA_C$ receptor-mediated inhibition across BC classes in rat and ferret (Euler & Wassle, 1998; Shields *et al.* 2000). These results predict that there may be differential receptor filtering of GABAergic light-evoked inhibitory postsynaptic currents (L-IPSCs) across the distinct parallel BC pathways. However, because the magnitude and shape of L-IPSCs depends not only on receptor type and distribution but also on their activation by neurotransmitter release, differences in receptor distribution may not correlate directly with differences in L-IPSCs. Since $GABA_C$ receptor-mediated responses have slow kinetics (Eggers & Lukasiewicz, 2006*b*), we expected that differences in $GABA_C$ receptor distributions would primarily shape the decay of L-IPSCs. Thus, we examined the decay of pharmacologically isolated GABAergic L-IPSCs across all classes of WT BCs (in the presence of strychnine) by determining the time at which the response decayed to 37% of its maximum (D_{37}). The GABAergic L-IPSCs (Fig. 1*A–C*) of rod BCs decayed slowest, followed by ON cone and then OFF cone BCs (Fig. 1*D*), suggesting that distinct proportions of $GABA_A$ and $GABA_C$ receptors shape light-evoked inhibition across BC classes.

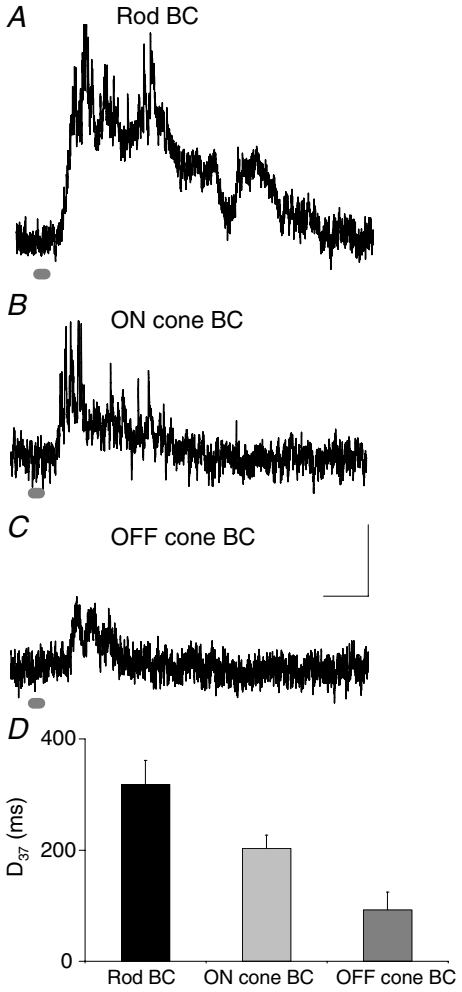

Figure 1. The kinetics of GABAergic light-evoked IPSCs (L-IPSCs) vary across WT bipolar cell (BC) class
L-IPSCs were recorded from BCs voltage clamped to 0 mV, the reversal potential for excitatory currents mediated by non-selective cation channels, and elicited with a 30 ms full field stimulus (dark grey bar). *A–C*, WT GABAergic L-IPSCs (recorded in the presence of strychnine) from rod, ON cone and OFF cone BCs, respectively. *D*, the decay of the L-IPSCs (D_{37}) varied by BC class with rod BCs (330.6 ± 38.1 ms, $n = 10$) significantly slower than either ON cone BCs (D_{37}, 203.0 ± 24.5 ms, $n = 7$) or OFF cone BC (D_{37}, 92.8 ± 31.6 ms, $n = 3$) (ANOVA, $P < 0.01$, rod *versus* ON $P < 0.05$; rod *versus* OFF, $P < 0.01$). ON cone BCs also had a slower D_{37} than OFF cone BCs ($P < 0.05$). Scale bars, 5 pA and 200 ms.

Proportions of $GABA_A$ and $GABA_C$ receptor-mediated inhibition vary with BC class

Differences in GABA release onto synaptic $GABA_A$ and $GABA_C$ receptors could also contribute to the decay of GABAergic L-IPSCs. To investigate how receptor properties and distributions shaped GABAergic responses in mouse retina, we by-passed release by directly activating presynaptic GABA receptors on morphologically identified WT BCs with focal GABA application onto the axon terminals (Shields *et al.* 2000). GABA-evoked currents were isolated by blocking glycine and ionotropic glutamate receptors, as noted in the Methods. $GABA_C$ and $GABA_A$ receptor-specific response components were separated with the antagonists bicuculline or TPMPA, respectively. The proportion of the total GABA-evoked current mediated by either $GABA_A$ or $GABA_C$ receptors differed across BC class (Fig. 2*Aa–Ca*). To quantify their contributions to the total current, we computed the ratio of the charge transfer (Q) for each isolated receptor (Q-$GABA_C$ or Q-$GABA_A$) to the total charge transfer obtained in control solution (Fig. 2*D*). In rod BCs (Fig. 2*Aa*), $GABA_C$ receptors mediated most of the GABA-evoked total current (0.87 ± 0.05, $n = 7$), with a small contribution from $GABA_A$ receptors (0.17 ± 0.07, $n = 12$; $GABA_C$ *versus* $GABA_A$ $P < 0.0001$, Fig. 2*D*). GABA-evoked currents in ON cone BC (Fig. 2*Ba*) were also dominated by $GABA_C$ receptors ($GABA_C$ 0.60 ± 0.03, $n = 15$; $GABA_A$ 0.29 ± 0.16, $n = 3$; $GABA_C$ *versus* $GABA_A$; $P < 0.005$), although the $GABA_C$ receptor-mediated proportion was significantly smaller than in rod BCs (ANOVA $P < 0.001$, Scheffé's *post hoc* test; $P < 0.05$; Fig. 2*D*). In OFF cone BCs (Fig. 2*Ca*), the $GABA_C$ receptor contribution was smallest

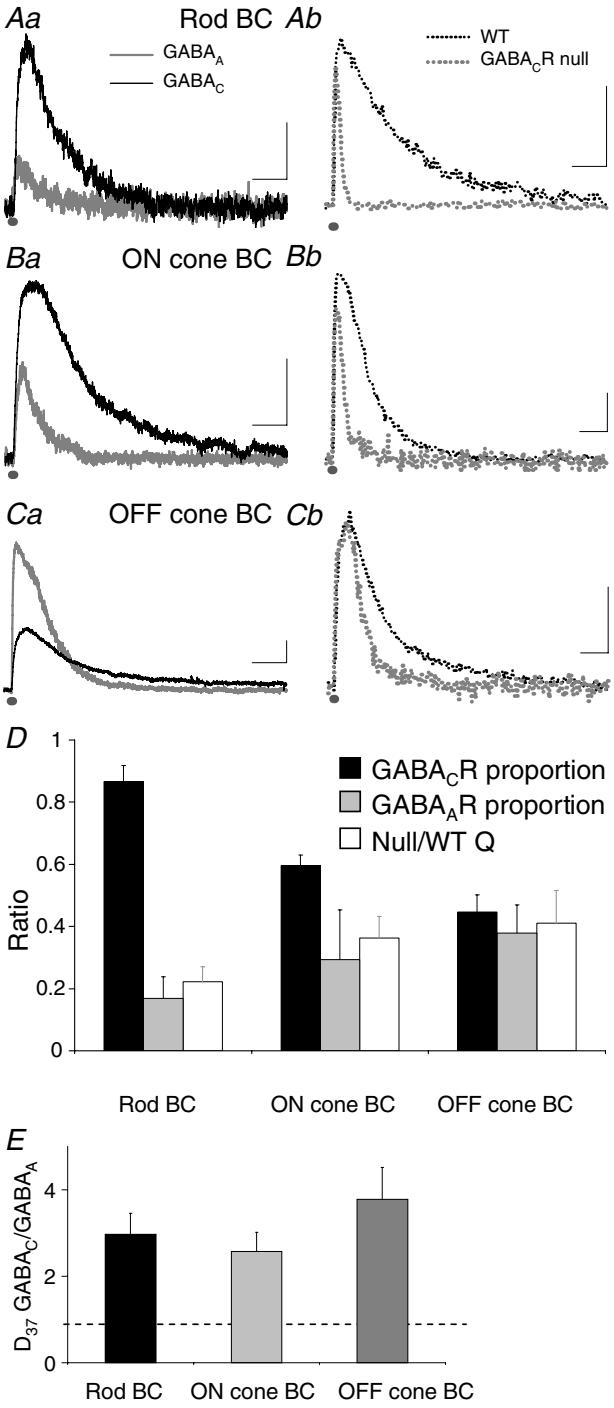

Figure 2. GABA$_A$ and GABA$_C$ contributions to GABA-evoked (30 μm) currents also vary across BC class
GABA$_A$ or GABA$_C$ receptor-mediated currents were isolated and measured using TPMPA or bicuculline, respectively, in WT rod (*Aa*), ON cone (*Ba*) and OFF cone (*Ca*) BCs. GABA-evoked currents from GABA$_C$R null rod (*Ab*), ON cone (*Bb*) and OFF (*Cb*) cone BCs compared with GABA-evoked currents from WT BCs of the same class. (The dark grey bar below each trace indicates the duration of the GABA puff that elicited the current.) *D*, fractional GABA-evoked current mediated by GABA$_A$ and GABA$_C$ receptors in WT BCs was calculated by normalizing GABA$_A$ and GABA$_C$ charge transfer (Q) to total Q. In WT rod and ON cone BCs, GABA$_C$ receptors (black bars) mediated significantly more of the total response (Q) than GABA$_A$ receptors (grey bars; $P < 0.001$ and 0.005, respectively). In WT OFF cone BCs the proportion of GABA$_A$ and GABA$_C$ contributions was similar ($P = 0.3$). For GABA$_C$R null BCs, the average Q of the GABA-evoked current was normalized to the average WT response (white bars), which gives an estimate of the contribution of GABA$_A$ receptors to the WT GABA-evoked current. In each BC class, this value is similar to the measured contribution of GABA$_A$ receptors (grey bars) to the WT current. In this histogram, the black error bars for GABA$_C$ (black) and GABA$_A$ (grey) represent the S.E.M. For Null/WT (white), the grey error bars represent the propagated error from the averages. *E*, in all BC classes, the GABA$_C$ receptor-mediated currents had slower decay times than the GABA$_A$ receptor-mediated currents ($P < 0.05$), indicated by the ratios of the average GABA$_C$ to GABA$_A$ decay (D_{37}) values being greater than 1. Scale bars: A, *B* and *Ca*, 20 pA; *Cb*, 10 pA, and 500 ms in all.

of all BC classes (GABA$_C$ = 0.45 ± 0.06, $n = 7$, rod *versus* OFF BC $P < 0.001$) and was similar to the contribution by GABA$_A$ receptors (GABA$_A$ = 0.38 ± 0.09, $n = 7$; GABA$_C$ *versus* GABA$_A$; $P = 0.3$). These findings are in general agreement with earlier studies in other species (Euler & Wassle, 1998; Shields *et al.* 2000), and they allow us to compare the properties of GABA-evoked and light-evoked IPSCs in the mouse.

To assess the contribution of GABA$_C$ and GABA$_A$ receptors to GABA-evoked current kinetics, we compared the decay times of the individual receptor-mediated currents in the same WT BCs. This approach minimizes any kinetic differences arising from variations in the distance between the puffer pipette and the axon terminals. The decays of WT GABA$_C$ receptor-mediated currents were longer than GABA$_A$ receptor-mediated currents in all BC classes, indicating that GABA$_C$ receptors determine the decay kinetics (Fig. 2*E*, $P < 0.05$). This is similar to observations made previously in mouse rod BCs (McCall *et al.* 2002), ferret BCs (Shields *et al.* 2000) and heterologous expression systems (Amin & Weiss, 1994). Furthermore, the correspondence in the decay ratios across BC classes suggests that the kinetic properties and, possibly, the receptor subunit composition of both GABA$_C$ and GABA$_A$ receptors are similar across BC classes.

To confirm distinct ratios of GABA$_A$ and GABA$_C$ receptors across BC class, we compared GABA-evoked currents from WT BCs and BCs from mice lacking GABA$_C$ ρ1 receptor subunits, which as a consequence lack retinal GABA$_C$ receptors (GABA$_C$R null) (McCall *et al.* 2002). We observed a large difference in rod BC GABA-evoked currents between WT and GABA$_C$R null mice (Fig. 2*Ab*). However, this difference diminished when we compared GABA-evoked currents in ON (Fig. 2*Bb*) and OFF cone (Fig. 2*Cb*) BCs. When we computed the ratio of average GABA-evoked charge transfer (Q) in GABA$_C$R null (GABA$_A$ only) to WT (GABA$_A$ + GABA$_C$) mice, we found that for each BC class (Fig. 2*D*), the

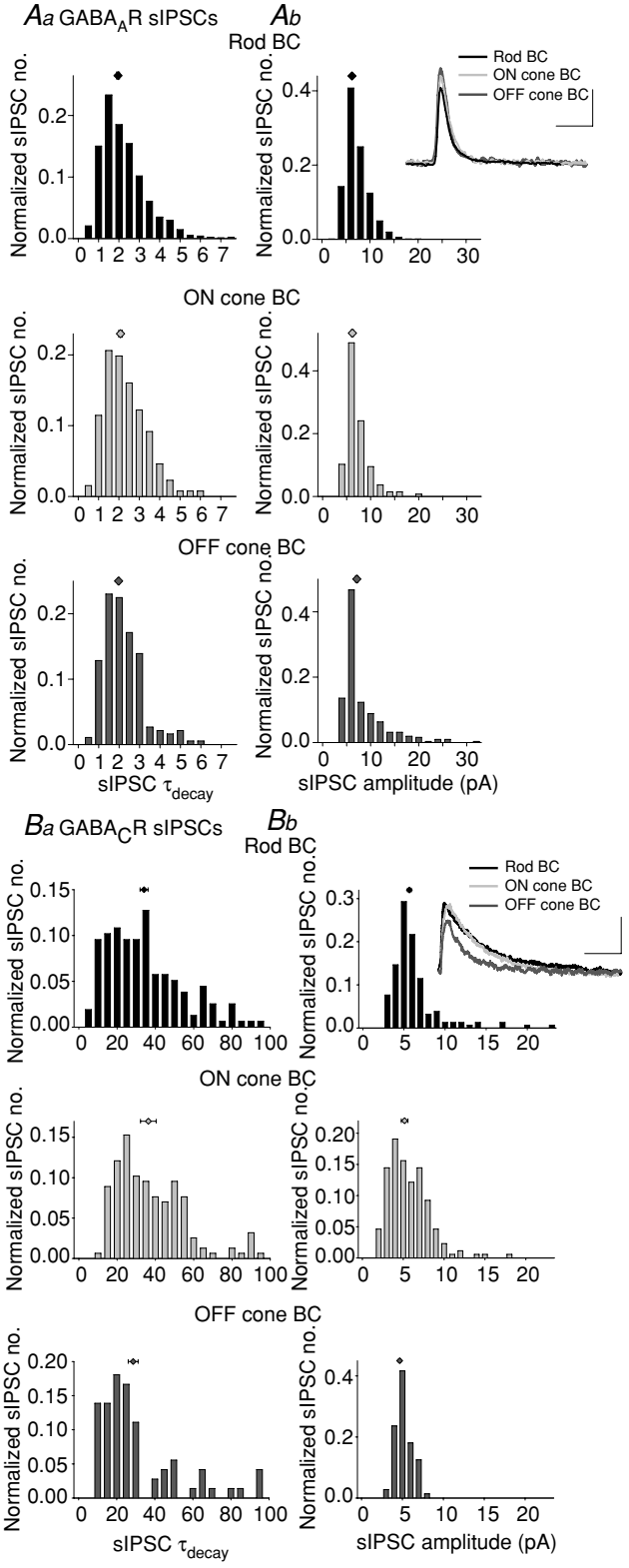

Figure 3. Analyses of spontaneous IPSCs (sIPCS) indicate that both GABA$_A$ and GABA$_C$ receptors are synaptically activated in all BC classes

A, normalized histograms showing distributions of τ_{decay} (left) and amplitude (right) for GABA$_A$ receptor-mediated sIPSCs recorded from rod (top, N = 972), ON cone (middle, N = 137) and OFF (bottom, N = 317) cone BCs (inset: average sIPSCs). Symbols (♦) denote the average values ± S.E.M. *Aa*, there were no significant differences among the τ_{decay} values for rod, ON cone and OFF cone BC GABA$_A$ sIPSCs (K–S, $P = 0.3$). *Ab*, GABA$_A$ sIPSCs from OFF cone BCs had significantly larger peak values (K–S, $P < 0.05$) than those from rod BCs. *B*, normalized histograms showing distributions of τ_{decay} and amplitude for GABA$_C$ receptor-mediated sIPSCs from rod (N = 157), ON cone (N = 173) and OFF cone BCs (N = 72) (inset: average sIPSCs), in the presence of kainate (10 μM). Conventions are the same as in *A*. *Ba*, the sIPSCs from OFF cone BCs had significantly shorter τ_{decay} than ON cone and rod BC sIPSCs (K–S, $P < 0.001$). *Bb*, the GABA$_C$ sIPSCs from OFF cone BCs had significantly smaller amplitudes than ON cone and rod BC GABA$_C$ sIPSCs (K–S, $P < 0.01$). Scale bars: *A*, 2 pA and 5 ms; *B*, 2 pA and 50 ms.

GABA$_C$R null : WT ratio (white bars) was comparable to the WT GABA$_A$: WT total ratio (black bars). This result is consistent with our previous observations that the GABA$_C$-mediated current is eliminated in retinal BCs and that there is no compensatory up-regulation of GABA$_A$ receptors in GABA$_C$R null rod BCs (McCall *et al.* 2002; Eggers & Lukasiewicz, 2006*a*; Sagdullaev *et al.* 2006). These results now extend our previous conclusions, as we show no compensatory up-regulation in any BC class.

Spontaneous GABA$_A$ and GABA$_C$ receptor-mediated IPSCs are observed in all BC classes

The GABA-evoked responses from WT and GABA$_C$R null BCs suggest that GABA$_A$ and GABA$_C$ receptor contributions vary across mouse BC classes. However, applied GABA activates receptors at both extrasynaptic and synaptic locations and not all of these receptors may be activated during synaptic transmission. To isolate and characterize synaptically activated GABA$_A$ and GABA$_C$ receptors across BC classes in a way that is largely independent of transmitter release and clearance, we recorded pharmacologically isolated GABA$_A$ and GABA$_C$ receptor-mediated spontaneous IPSCs (sIPSCs). Differences in sIPSC decay should reflect differences in receptor subunit composition, while differences in sIPSC amplitudes should reflect differences in synaptic receptor cluster size. The decay times (τ_{decay}) of GABA$_A$ receptor-mediated sIPSCs were similar across all three BC classes (Fig. 3*Aa*). In contrast, their amplitudes differed: GABA$_A$ receptor-mediated sIPSCs in OFF cone BC were significantly larger than in rod BCs (Fig. 3*Ab*) (Table 1, K–S, $P < 0.05$).

GABA$_C$ receptor-mediated sIPSCs are difficult to record, but can be observed if spontaneous GABA release is increased by including kainate in the bath (10 μM) (Frech & Backus, 2004; Eggers & Lukasiewicz, 2006*b*). Across all BC classes, the decay of GABA$_C$ receptor-mediated sIPSCs was significantly longer than GABA$_A$ receptor-mediated sIPSCs (Table 1, K–S, $P < 0.001$). We also observed a

Table 1. Parameters for sIPSCs

BC cell	$GABA_C$ amp (pA)	$GABA_C$ τ_{decay} (ms)	N	$GABA_A$ amp (pA)	$GABA_A$ τ_{decay} (ms)	N	Glycine amp (pA)	Glycine τ_{decay} (ms)	N
OFF	4.7 ± 0.2	28.6 ± 2.6	72	7.1 ± 0.4	2.0 ± 0.5	317	21.9 ± 0.7	3.7 ± 0.5	1088
ON	5.2 ± 0.4	36.3 ± 4.1	173	6.2 ± 0.4	2.1 ± 0.5	137	NA	NA	NA
Rod	5.7 ± 0.2	34.1 ± 2.1	157	6.2 ± 0.4	2.0 ± 0.5	972	10.1 ± 0.4	3.6 ± 0.5	193

small but significant difference in the decay of $GABA_C$ receptor-mediated sIPSCs between OFF cone BCs and ON cone or rod BCs (Fig. 3*Ba*; Table 1, K–S, $P < 0.001$ for both comparisons). Consistent with our observations of GABA-evoked currents, the amplitudes of $GABA_C$ receptor-mediated sIPSCs from OFF cone BCs were smaller than those from either ON cone or rod BCs (Fig. 3*Bb*, K–S, $P < 0.01$). Additionally, the amplitudes of $GABA_A$ and $GABA_C$ receptor-mediated sIPSCs were similar in rod BCs, while the amplitudes of $GABA_A$ receptor-mediated sIPSCs in both ON and OFF cone BCs were significantly larger than their respective $GABA_C$ sIPSCs (Table 1, K–S, $P < 0.001$).

These results show that $GABA_A$ and $GABA_C$ receptors can be activated synaptically in all BC classes. The similarities in decay times suggest that the subunit compositions of $GABA_A$ and $GABA_C$ receptors may be similar across BC classes. However, differences in sIPSC amplitudes suggest that $GABA_A$ receptor synaptic clusters should be the largest on OFF cone BCs, while $GABA_C$ receptor synaptic clusters should be largest on rod BC. These findings suggest that synaptic receptor properties play a role in shaping the L-IPSC. Rod BC responses are predominantly shaped by $GABA_C$ receptors, while $GABA_A$ receptors primarily shape OFF cone BC responses. In ON cone BC responses, $GABA_A$ and $GABA_C$ receptors play a more balanced role.

Pharmacologically isolated $GABA_A$ and $GABA_C$ receptor-mediated L-IPSCs vary with BC class

The relatively small differences found in sIPSCs across BC class were inconsistent with the much larger differences in light-evoked currents, suggesting that synapse distribution and GABA release may be more important than receptor cluster size in shaping GABAergic L-IPSCs. To characterize the light-evoked activation of GABA receptors, we recorded and compared pharmacologically isolated $GABA_A$ and $GABA_C$ receptor-mediated L-IPSCs across the three BC classes (Fig. 4*A–C*). When pharmacologically

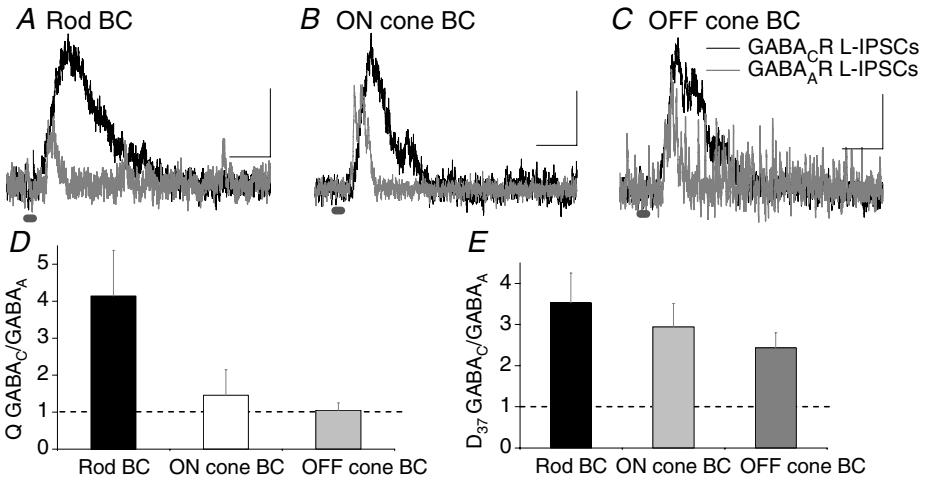

Figure 4. $GABA_A$ and $GABA_C$ receptors differentially contribute to L-IPSCs across BC classes
Representative L-IPSCs (dark grey bar light stimulus duration 30 ms) mediated by $GABA_C$ and $GABA_A$ receptors from rod BCs (*A*), ON cone BCs (*B*) and OFF cone BCs (*C*). Scale bars, 5 pA and 200 ms. *D*, the histogram plots average *Q* of $GABA_C$ receptor-mediated L-IPSCs normalized to the *Q* of $GABA_A$ L-IPSCs for each BC class. $GABA_C$ receptor-mediated L-IPSCs were significantly larger than $GABA_A$ L-IPSCs in rod BCs ($GABA_A$, $n = 12$; $GABA_C$, $n = 14$, $P < 0.01$) but there was no significant difference in $GABA_C$ and $GABA_A$ L-IPSC *Q* for ON ($GABA_A$, $n = 13$; $GABA_C$, $n = 5$) or OFF cone BCs ($GABA_A$, $n = 7$; $GABA_C$, $n = 5$). *E*, the histogram plots the average L-IPSC decay (D_{37}) of $GABA_C$ receptor-mediated normalized to the average $GABA_A$ L-IPSC D_{37} for each BC class. $GABA_C$ receptor-mediated currents were significantly longer than $GABA_A$ current in every class (rod, $P < 0.001$; ON, $P < 0.01$; OFF, $P < 0.05$). Error bars in *D* and *E* represent propagated standard errors of the average $GABA_A$ and $GABA_C$ values.

Table 2. Parameters for L-IPSCs from Rod BCs

L-IPSC type	D_{37} (ms)	Q (fC)	Peak (pA)	Time to peak (ms)	n
$GABA_A$	134.1 ± 35.5	954 ± 371	7.1 ± 1.2	158.9 ± 12.5	12
$GABA_C$	472.4 ± 82.7	3950 ± 682	10.4 ± 1.4	225.7 ± 17.9	14
Glycine	279.1 ± 28.9	1635 ± 421	10.6 ± 1.6	154.0 ± 17.5	13
WT control	275.3 ± 19.8	3215 ± 368	13.5 ± 1.3	168.2 ± 9.2	43
$GABA_C$R null control	119.6 ± 14.3	1775 ± 559	13.1 ± 2.2	156.7 ± 8.9	15

Table 3. Parameters for L-IPSCs from ON cone BCs

L-IPSC type	D_{37} (ms)	Q (fC)	Peak (pA)	Time to peak (ms)	n
$GABA_A$	87.8 ± 19.4	1972 ± 1077	13.7 ± 2.6	136.3 ± 5.8	13
$GABA_C$	242.5 ± 52.0	2877 ± 462	14.0 ± 1.8	207 ± 21.3	5
WT control	148.9 ± 10.7	2172 ± 400	16.3 ± 3.2	133.4 ± 6.7	17
$GABA_C$R null control	101.0 ± 16.5	1385 ± 533	19.6 ± 4.2	132.2 ± 8.4	7

Table 4. Parameters for L-IPSCs from OFF cone BCs

L-IPSC type	D_{37} (ms)	Q (fC)	Peak (pA)	Time to peak	n
$GABA_A$	163.5 ± 8.6	3081 ± 846	10.0 ± 3.6	157.9 ± 22.4	7
$GABA_C$	397.4 ± 79.6	3225 ± 261	14.5 ± 4.0	260.7 ± 39.6	5
Glycine	280.0 ± 30.2	12204 ± 3448	65.1 ± 19.5	136.8 ± 16.5	7
WT control	253.8 ± 27.1	22770 ± 5474	108.0 ± 19.9	157.3 ± 30.3	13
$GABA_C$R null control	238.9 ± 32.0	16821 ± 7885	45.8 ± 19.7	164.1 ± 37.8	6

isolating $GABA_C$ receptors with bicuculline, we probably blocked the influence of serial inhibitory circuits on the $GABA_A$ and $GABA_C$ receptor-mediated inputs to BCs. Thus, these responses should reflect the maximal $GABA_C$ receptor-mediated input, as we previously described for rod BCs (Eggers & Lukasiewicz, 2006*a*).

Rod BCs received the most light-evoked input via $GABA_C$ receptors with a smaller contribution via $GABA_A$ receptors (Fig. 4*A* and *D*, Table 2, $P < 0.01$) (Eggers & Lukasiewicz, 2006*b*). Both $GABA_A$ and $GABA_C$ receptors mediated L-IPSCs of similar magnitude in ON (Table 3, $P = 0.5$) and OFF cone BCs (Table 4, $P = 0.9$), so the relative contribution of $GABA_C$ receptor-mediated input in these two classes was smaller than in rod BCs (Fig. 4*D*). Across all BC classes, $GABA_C$ receptor-mediated L-IPSCs had slower decay times, as we observed for GABA-evoked currents and sIPSCs, as well as slower times to peak than $GABA_A$ receptor-mediated L-IPSCs (Fig. 4*E*, Tables 2–4, $P < 0.05$). However, we found no significant differences across the BC classes in $GABA_A$ L-IPSC decay times or times to peak (ANOVAs: decay, $GABA_A$, $P > 0.2$; time to peak, $GABA_A$, $P > 0.2$) or in $GABA_C$ receptor-mediated L-IPSC decay times or times to peak (ANOVAs: decay, $GABA_C$, $P > 0.2$; time to peak, $GABA_C$, $P > 0.5$). Taken together, these results suggest that the kinetics of the $GABA_A$ and $GABA_C$ receptor-mediated L-IPSCs were similar across BC classes, but the relative $GABA_A$ and $GABA_C$ receptor contributions vary. While the similarity between the decay (D_{37}) of the total GABAergic (Fig. 1) and $GABA_A$ receptor-mediated L-IPSCs in OFF cone BCs (Table 4) suggests a primary role for $GABA_A$ receptors, this idea is not consistent with our observation of a significant $GABA_C$ receptor-mediated contribution to sIPSCs (Fig. 3) and L-IPSCs (Fig. 4) in OFF cone BCs. One potential explanation for this discrepancy is that $GABA_A$ receptor-mediated serial inhibition, among GABAergic amacrine cells, differentially suppresses $GABA_C$ receptor-mediated inputs (Zhang *et al.* 1997; Roska *et al.* 1998; Eggers & Lukasiewicz, 2006*a*).

Serial connections mediated by $GABA_A$ receptors suppress $GABA_C$ receptor-mediated L-IPSCs

To determine whether $GABA_A$ receptor-mediated serial inhibition is present across BC classes, we recorded GABAergic L-IPSCs and compared them to L-IPSCs recorded in the presence of bicuculline, when serial GABAergic signalling between amacrine cells was eliminated. Strychnine, which does not disrupt these serial connections (Eggers & Lukasiewicz, 2006*a*), was always present to isolate the GABAergic L-IPSCs. The addition of bicuculline increased the L-IPSC charge transfer (Q) across all the BC classes (Fig. 5*A*–*D*, ANOVA, $P = 0.4$). This suggests that $GABA_C$ receptor-mediated inputs to all BC classes were similarly suppressed by $GABA_A$ receptor-mediated serial inhibition.

$GABA_C$ receptors shape L-IPSCs to rod and ON cone BCs but not OFF cone BCs

Since $GABA_C$ receptor-mediated inputs can be controlled by serial inhibition, our measures of the pharmacologically isolated $GABA_C$ receptor-mediated L-IPSCs may be overestimates of the $GABA_C$ receptor-mediated input to the total L-IPSCs. To estimate the $GABA_C$ receptor contribution when serial inhibition was present, we compared GABAergic L-IPSCs across BC classes from WT and $GABA_C$R null mice. The slow decay kinetics of WT $GABA_C$ receptor-mediated L-IPSCs (Fig. 4) predicts that L-IPSCs from $GABA_C$R null BCs will decay faster than WT BCs in any BC class with a significant $GABA_C$ receptor-mediated input. Consistent with this hypothesis, we found that the decay of L-IPSCs from $GABA_C$R null rod (Fig. 6*A* and *D*; $P < 0.0001$, Table 2) (Eggers & Lukasiewicz, 2006*b*) and ON cone BCs was significantly briefer than WT (Fig. 6*B* and *D*; $P < 0.05$, Table 3). In OFF cone BCs, by contrast, the decay of L-IPSCs from WT and $GABA_C$R null were similar (Fig. 6*C* and *D*; $P = 0.7$, Table 4), suggesting little or no $GABA_C$ receptor-mediated contribution when serial inhibition was present. Together our results from GABA-evoked currents and L-IPSCs show that there is a gradient of $GABA_C$ receptor-mediated input across BC classes and that this input proportionately prolongs the timecourse of GABAergic L-IPSCs.

Glycinergic inhibition is the dominant component of inhibition in OFF cone BCs

As many BCs also receive glycinergic inhibition (Eggers & Lukasiewicz, 2006*b*; Ivanova *et al.* 2006), we compared the properties of pharmacologically isolated glycinergic sIPSCs in rod and OFF BCs. Glycine receptor-mediated sIPSCs were never observed in ON cone BCs, consistent with previous observations (Ivanova *et al.* 2006). Figure 7*A* and *B* shows the distributions of decay (τ_{decay}) and amplitude of glycinergic sIPSCs for OFF cone and rod BCs, as well as average glycinergic sIPSCs (inset). Rod and OFF cone BCs had similar decays, but the amplitude of glycine sIPSCs was significantly larger in OFF cone BCs (Table 1, K–S, $P < 0.0001$), suggesting that subunit composition was similar, but receptor cluster size differed in these two BC classes. The decay of glycine receptor-mediated sIPSCs also was significantly briefer than $GABA_C$ receptor-mediated sIPSCs (K–S, $P < 0.001$) and significantly longer than $GABA_A$ receptor-mediated sIPSCs (K–S, $P < 0.001$) in both rod and OFF cone BCs.

To determine if these differential contributions in glycinergic sIPSCs contributed to light-evoked inhibition, we recorded and characterized glycinergic L-IPSCs. As we observed with glycinergic sIPSCs, we found no light-evoked glycinergic input to ON cone bipolar cells. L-IPSC responses (Q) (Fig. 7*C*) in OFF cone BCs were significantly larger than in rod BCs (Fig. 7*D*, $P < 0.05$, Tables 2–4). Furthermore, glycinergic L-IPSCs were significantly larger than $GABA_A$ or $GABA_C$ receptor-mediated inputs in OFF cone BCs (Table 4, $P < 0.05$). Although the kinetics of glycine receptor-mediated sIPSCs are significantly faster than $GABA_C$ receptor-mediated sIPSCs, their L-IPSCs have similar decay kinetics ($P > 0.05$, Tables 2 and 4), probably

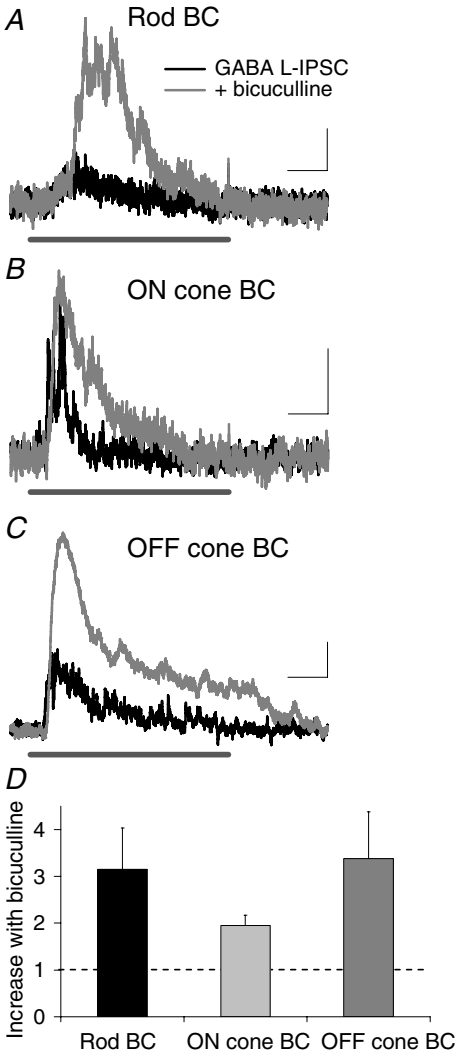

Figure 5. Serial inhibition mediated by $GABA_A$ receptors decreases $GABA_C$ receptor-mediated L-IPSCs in all WT BC classes
A–C, representative GABAergic L-IPSCs recorded from WT rod (*A*, $n = 9$), ON cone (*B*, $n = 7$) and OFF cone (*C*, $n = 6$) BCs evoked by a light stimulus (1000 ms duration; dark grey bar) in the presence of strychnine (black trace) and when $GABA_A$-mediated inhibition is blocked (strychnine + bicuculline, isolated $GABA_C$ receptor-mediated L-IPSCs). *D*, the histogram plots the average L-IPSC Q in the presence of strychnine + bicuculline normalized to the Q only in the presence of strychnine (dashed line). All WT BC classes showed a significant increase when $GABA_A$ input was blocked and there was no significant difference in proportional increase across BC class (ANOVA, $P = 0.4$). Scale bars: *A*, 5 pA; *B* and *C*, 10 pA, and 200 ms in all.

attributable to prolonged light-evoked glycine release (Eggers & Lukasiewicz, 2006*b*). These results suggest that glycine receptor-mediated inputs dominate L-IPSCs in OFF cone BCs in dark-adapted conditions.

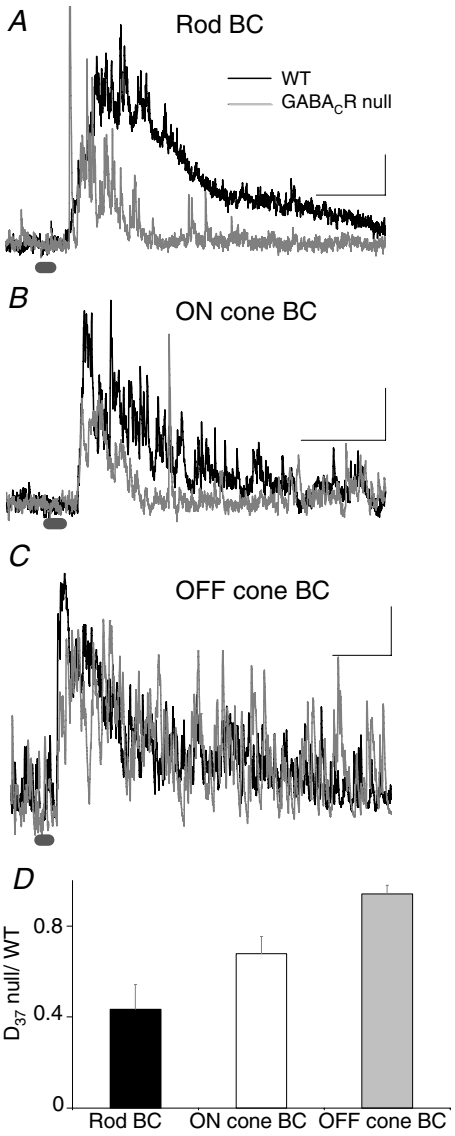

Figure 6. GABA$_C$ receptors shape L-IPSCs in ON cone and rod BCs, but not OFF cone BCs
A–C, representative L-IPSCs (30 ms light stimulus duration, grey bar) from rod (*A*; adapted from Eggers & Lukasiewicz, 2006*b*), ON cone (*B*) and OFF cone (*C*) BCs in WT (black) and GABA$_C$R null (grey) mice. *D*, the histogram plots the average L-IPSCs decay (D_{37}) from GABA$_C$R null BCs normalized to WT. GABA$_C$R null L-IPSCs in rod BCs (WT, $n = 43$; null, $n = 15$, $P < 0.0001$) and ON cone BCs (WT, $n = 17$; null, $n = 4$, $P < 0.05$) were significantly briefer than WT. There was no significant difference in L-IPSC decays from GABA$_C$R null and WT OFF cone BCs (WT, $n = 13$; null, $n = 6$, $P = 0.7$). Scale bars: *A* and *B*, 5 pA; *C*, 30 pA, and 200 ms in all. Error bars in *D* represent propagated standard errors of the average null to WT values.

The decay of combined glycinergic and GABAergic L-IPSCs varies with BC class

We have shown that the relative contributions of isolated glycine, GABA$_A$ and GABA$_C$ receptor-mediated inputs vary across BC class. To examine how the combination of these receptor-mediated inputs shape the total L-IPSCs, we compared their decay times (D_{37}) across different WT BC classes (Fig. 8*A–C*). The decay of L-IPSCs in rod BCs was significantly slower than ON cone BCs (ANOVA. $P < 0.001$; Scheffé's *post hoc* test, rod *versus* ON cone BC; $P < 0.001$, Fig. 8*D*, Tables 2 and 3), consistent with our results showing that GABA$_C$ receptor-mediated input was greater in rod than ON cone BCs. Despite the relative lack of GABA$_C$ receptor-mediated input to OFF cone BCs, the decay (D_{37}) of rod and OFF cone BCs was similar (Scheffé's *post hoc* test, $P = 0.8$, Fig. 8*D*, Table 4). The slow decay of L-IPSCs in OFF cone BCs was attributable to their large glycinergic input, as their total L-IPSCs were significantly longer than their GABAergic L-IPSCs (Figs 8*D* and 1*D*, respectively; $P < 0.01$). These results suggest that under dark-adapted conditions, GABA$_C$ receptor-mediated inputs are important for determining the timecourse of rod and ON cone BC L-IPSCs, but glycine receptor-mediated inputs predominate in OFF cone BCs.

Discussion

Using pharmacological tools and a mouse lacking retinal GABA$_C$ receptors, we have found that both GABAergic and glycinergic presynaptic inhibition differ with BC class in dark-adapted conditions. Distinct contributions of slow GABA$_C$ receptor-mediated inputs determined the decay time of GABAergic L-IPSCs in different BC classes. Rod BCs, with large GABA$_C$ receptor-mediated contributions, exhibited the slowest GABAergic L-IPSC decays and OFF cone BCs with small GABA$_C$ receptor-mediated contributions exhibited the fastest decays. Glycinergic inputs also differentially contributed to inhibition across BC classes. Glycinergic inputs are absent in ON cone BC responses and most prominent in the responses of OFF cone BCs, where they mediated a slow inhibition, similar to that of GABA$_C$ receptors in other BC classes.

Functional significance of the variance in presynaptic inhibition across BC classes

Excitatory responses to photoreceptor input have distinct kinetics across BC classes (Awatramani & Slaughter, 2000; Li & DeVries, 2006). Rod-mediated responses have slower rise and decay kinetics than cone-mediated responses (Schnapf & Copenhagen, 1982; Cadetti *et al.* 2005). Li & Devries (2006) show that when cones are electrically stimulated, by-passing phototransduction, ON

cone BC responses have slower kinetics than OFF cone BC responses, suggesting that distinct postsynaptic glutamate receptors (Slaughter & Miller, 1981, 1983) shape ON and OFF bipolar cell responses. Consistent with this idea, ON and OFF cone BC light-evoked responses in the turtle retina showed distinct kinetics (Ashmore & Copenhagen, 1980). Experiments in the mammalian retina are still needed to demonstrate physiological differences of light-evoked excitatory responses in ON and OFF cone bipolar cells. Our data suggest that these distinct kinetics of the excitatory responses across BC class are well matched by the distinct kinetics of inhibition mediated by varying contributions of $GABA_C$ receptors across BC class. Although OFF cone BCs received little $GABA_C$ receptor-mediated input, their L-IPSCs still decay slowly in dark-adapted conditions because they are dominated by slowly decaying glycinergic inhibition.

We do not believe that this apparent difference is a mismatch between excitatory inputs and presynaptic inhibition in OFF cone BCs. Under the dark-adapted conditions used in our experiments, glycinergic inputs to OFF cone BCs arise primarily from AII amacrine cells, which are activated by signalling through the rod pathway (Strettoi *et al.* 1990). This OFF BC glycinergic input suppresses glutamate release and functions as the rod-mediated 'OFF' signal to OFF ganglion cells. Thus, the slow decay of glycinergic presynaptic inhibition in OFF cone BCs is actually well-matched to the slow timecourse of rod pathway excitation. In our previous experiments, we estimated the timecourse of glycine release, using a deconvolution analysis of rod BC L-IPSCs (Eggers & Lukasiewicz, 2006*b*), and showed that the slow decay kinetics of glycinergic L-IPSCs arise from prolonged release of glycine onto BCs. The similar kinetics of glycinergic L-IPSCs and sIPSCs in rod and OFF cone BCs (Tables 1, 2 and 4) suggests a similar, prolonged glycine release from AII amacrine cells to OFF cone BCs.

In contrast, under cone-mediated, light-adapted conditions AII amacrine cells receive only minor excitatory inputs (Protti *et al.* 2005; Trexler *et al.* 2005), resulting in little glycinergic input to OFF cone BCs. In the absence of this significant glycinergic input, our data predict that GABA-mediated inhibition most probably shapes L-IPSCs. Thus, our isolated GABAergic L-IPSCs approximate light-adapted responses and show a faster decay that reflects a large $GABA_A$ and a small $GABA_C$ receptor contribution. Under these conditions, cone-mediated responses of OFF cone BCs are again well

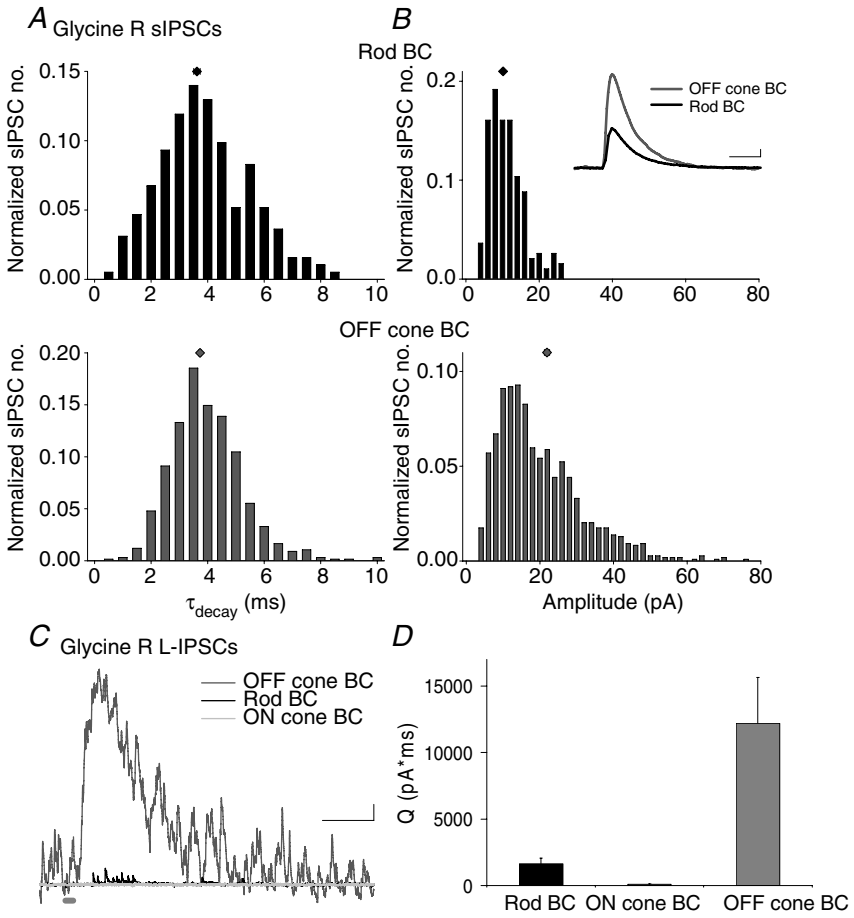

Figure 7. Glycine receptor-mediated inputs dominate L-IPSCs in OFF cone BCs
Glycine receptor-mediated sIPSCs were recorded from rod (black) OFF cone (dark grey), but not ON cone BCs. *A*, normalized histograms, with averages (♦) showing distributions of τ_{decay} for glycine sIPSCs. There was no significant difference between the τ_{decay} for OFF cone ($n = 1088$) and rod BC ($n = 193$) sIPSCs (K–S, $P = 0.8$). *B*, normalized histograms, showing distributions of peak amplitudes of glycine sIPSCs from rod and OFF cone BCs. The peak amplitude of glycine sIPSCs from OFF cone BCs were significantly larger than rod BCs (K–S, $P < 0.0001$). Inset, average glycine receptor-mediated sIPSCs. *C*, representative glycine receptor-mediated L-IPSCs (30 ms light stimulus, dark grey bar) recorded in both OFF cone ($n = 7$) and rod ($n = 13$) BCs. No light-evoked glycine receptor-mediated response was ever recorded in ON cone BCs ($n = 5$). *D*, the histogram plots glycine receptor-mediated L-IPSCs (*Q*) from rod (black) and OFF (grey) cone BCs. OFF cone L-IPSCs were significantly larger than rod and ON cone BCs ($P < 0.05$, the bar for ON cone BCs represents the baseline current). Rod BCs also had significantly more glycinergic input than ON cone BCs ($P < 0.01$). Scale bars: *B*, 2 pA and 5 ms; *C*, 10 pA and 200 ms.

matched to their presynaptic inhibition. Furthermore, this implies that the timecourse of presynaptic inhibition in OFF cone BCs depends on whether rod or cone signals are processed: slow glycinergic inputs matched to the slow rod input and fast GABA inputs matched to the brisk cone input.

Our findings may also explain the functional differences that we have observed between ON and OFF ganglion cell responses elicited via stimulation of cone pathways (Sagdullaev *et al.* 2006). When $GABA_C$ receptor-mediated input is eliminated, signalling in ON, but not in OFF ganglion cells is enhanced, suggesting that $GABA_C$ receptors only modulate ON BC output. However, immunocytochemical evidence indicates that $GABA_C$ receptors are expressed in both the ON and OFF sublaminae of the IPL (Interplexiform layer) (Enz *et al.* 1996; Shields *et al.* 2000; McCall *et al.* 2002), challenging the notion of differential $GABA_C$ receptor-mediated presynaptic inhibition. Our results demonstrate that $GABA_C$ receptor-mediated inhibition occurs in both ON and OFF cone BCs (Figs 3–5), but its magnitude differs between the two pathways (Figs 2, 3 and 6). Comparisons of GABA- and light-evoked currents from WT and $GABA_C$R null BCs indicate that $GABA_C$ receptors contributed significantly to ON cone BC responses, but their contribution to OFF cone BC responses was minor, at best. GABA-evoked currents showed a larger complement of $GABA_C$ receptors on OFF cone BCs than indicated by our L-IPSC results. This difference might be attributable to extrasynaptic $GABA_C$ receptors on OFF cone BCs, or to synaptic inputs that were limited by serial inhibitory circuits between amacrine cells (Zhang *et al.* 1997; Roska *et al.* 1998; Eggers & Lukasiewicz, 2006*a*).

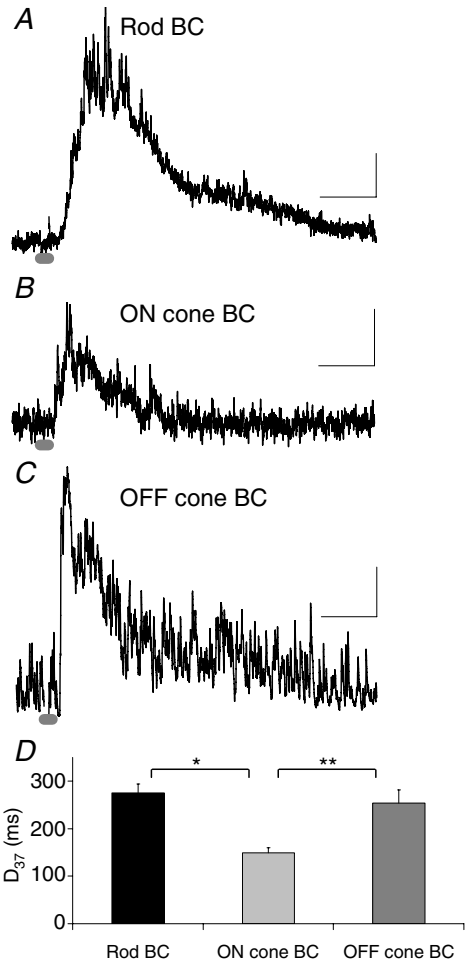

Figure 8. The decay of combined glycinergic and GABAergic L-IPSCs varies with WT BC class
A–C, representative total L-IPSCs (glycinergic + GABAergic) from rod (*A*), ON cone (*B*) and OFF cone (*C*) BCs evoked by a light stimulus (30 ms light stimulus, dark grey bar). *D*, the histogram plots the average decay (D_{37}) from each BC class. L-IPSCs from rod BCs were significantly slower than ON cone BCs (rod, $n = 43$; ON cone, $n = 17$, ANOVA, $P < 0.001$, rod *versus* ON Scheffé's *post hoc*, $^*P < 0.001$), but similar to OFF cone BCs ($n = 13$, $P = 0.86$). The decay of L-IPSCs from OFF cone BCs also was significantly slower than ON cone BCs ($^{**}P < 0.05$). Scale bars: *A* and *B*, 5 pA; *C*, 30 pA, and 200 ms in all.

Additionally, in the present study we have described the differences only between the major classes of BCs: rod, ON and OFF cone BCs. The ON and OFF ganglion cell pathway differences in $GABA_C$ receptor-mediated inhibition observed in all ON and OFF ganglion cell subtypes (Sagdullaev *et al.* 2006), suggests that similar differences occur in all ON and OFF cone bipolar cell types. We morphologically classified our BCs according to the scheme described by Ghosh *et al.* (2004) and found that $GABA_C$ receptor contributions fell into three categories, corresponding to rod, ON and OFF cone BCs. Although our conclusions are consistent with the major BC classifications, our sample sizes for different subtypes were insufficient to make conclusions about significant differences between subtypes. Thus, future studies may show differences within BC classes.

Temporally tuning inhibition with distinct inhibitory receptors

Similar to our observations of differential activation of $GABA_C$ receptors in the retina, temporal filtering through the expression of distinct inhibitory receptors also occurs in other areas of the CNS. In spinal cord and brainstem, the timecourse of IPSCs is temporally tuned by the relative activation of glycine and $GABA_A$ receptors with distinct kinetics (Jonas *et al.* 1998; O'Brien & Berger, 1999). In the hippocampus, the timecourses of inhibition and excitation mirror each other, and are controlled by distinct combinations of $GABA_A$ receptor subunits in different populations of interneurons (Hajos & Mody, 1997). Temporal tuning of inhibition is also important during development in many areas of the CNS. The decrease in the decay time of GABAergic IPSCs, attributable to changes

in GABA receptor subunit composition (Brickley *et al.* 1996; Dunning *et al.* 1999; Okada *et al.* 2000) parallels the decrease in the timecourse of excitation (Takahashi, 2005).

Our findings demonstrate that distinct forms of presynaptic inhibition in parallel retinal BC pathways are attributable to different complements of GABA and glycine receptors. The timecourse of presynaptic inhibitory inputs generally matches excitatory inputs to distinct BCs reported in the literature, which are temporally filtered by different glutamate receptors types (Ashmore & Copenhagen, 1980; Schnapf & Copenhagen, 1982; Cadetti *et al.* 2005; Li & DeVries, 2006). Balancing the timecourses of excitation and presynaptic inhibition across parallel bipolar cell channels ensures that separate signals are transmitted effectively to their ganglion cell targets. This may be a strategy used both in the retina and elsewhere in the CNS to coordinate the inputs and outputs of neurons involved in parallel information processing.

References

Amin J & Weiss DS (1994). Homomeric rho 1 GABA channels: activation properties and domains. *Receptors Channels* **2**, 227–236.

Ashmore JF & Copenhagen DR (1980). Different postsynaptic events in two types of retinal bipolar cell. *Nature* **288**, 84–86.

Awatramani GB & Slaughter MM (2000). Origin of transient and sustained responses in ganglion cells of the retina. *J Neurosci* **20**, 7087–7095.

Brickley SG, Cull-Candy SG & Farrant M (1996). Development of a tonic form of synaptic inhibition in rat cerebellar granule cells resulting from persistent activation of $GABA_A$ receptors. *J Physiol* **497**, 753–759.

Cadetti L, Tranchina D & Thoreson WB (2005). A comparison of release kinetics and glutamate receptor properties in shaping rod–cone differences in EPSC kinetics in the salamander retina. *J Physiol* **569**, 773–788.

Chadderton P, Margrie TW & Hausser M (2004). Integration of quanta in cerebellar granule cells during sensory processing. *Nature* **428**, 856–860.

Dong C & Werblin FS (1998). Temporal contrast enhancement via $GABA_C$ feedback at bipolar terminals in the tiger salamander retina. *J Neurophysiol* **79**, 2171–2180.

Dunning DD, Hoover CL, Soltesz I, Smith MA & O'Dowd DK (1999). $GABA_A$ receptor-mediated miniature postsynaptic currents and alpha-subunit expression in developing cortical neurons. *J Neurophysiol* **82**, 3286–3297.

Eggers ED & Lukasiewicz PD (2006*a*). $GABA_A$, $GABA_C$ and glycine receptor-mediated inhibition differentially affects light-evoked signalling from mouse retinal rod bipolar cells. *J Physiol* **572**, 215–225.

Eggers ED & Lukasiewicz PD (2006*b*). Receptor and transmitter release properties set the time course of retinal inhibition. *J Neurosci* **26**, 9413–9425.

Enz R, Brandstätter JH, Wässle H & Bormann J (1996). Immunocytochemical localization of the $GABA_C$ receptor ρ subunits in the mammalian retina. *J Neurosci* **16**, 4479–4490.

Euler T & Masland RH (2000). Light-evoked responses of bipolar cells in mammalian retina. *J Neurophysiol* **83**, 1817–1829.

Euler T & Wassle H (1998). Different contributions of $GABA_A$ and $GABA_C$ receptors to rod and cone bipolar cells in a rat retinal slice preparation. *J Neurophysiol* **79**, 1384–1395.

Frech MJ & Backus KH (2004). Characterization of inhibitory postsynaptic currents in rod bipolar cells of the mouse retina. *Vis Neurosci* **21**, 645–652.

Ghosh KK, Bujan S, Haverkamp S, Feigenspan A & Wassle H (2004). Types of bipolar cells in the mouse retina. *J Comp Neurol* **469**, 70–82.

Hajos N & Mody I (1997). Synaptic communication among hippocampal interneurons: properties of spontaneous IPSCs in morphologically identified cells. *J Neurosci* **17**, 8427–8442.

Ivanova E, Muller U & Wassle H (2006). Characterization of the glycinergic input to bipolar cells of the mouse retina. *Eur J Neurosci* **23**, 350–364.

Jonas P, Bischofberger J & Sandkuhler J (1998). Corelease of two fast neurotransmitters at a central synapse. *Science* **281**, 419–424.

Li W & DeVries SH (2006). Bipolar cell pathways for color and luminance vision in a dichromatic mammalian retina. *Nat Neurosci* **9**, 669–675.

Lukasiewicz PD & Roeder RC (1995). Evidence for glycine modulation of excitatory synaptic inputs to retinal ganglion cells. *J Neurosci* **15**, 4592–4601.

Lukasiewicz PD & Werblin FS (1994). A novel GABA receptor modulates synaptic transmission from bipolar to ganglion and amacrine cells in the tiger salamander retina. *J Neurosci* **14**, 1213–1223.

McCall MA, Lukasiewicz PD, Gregg RG & Peachey NS (2002). Elimination of the $\rho 1$ subunit abolishes $GABA_C$ receptor expression and alters visual processing in the mouse retina. *J Neurosci* **22**, 4163–4174.

O'Brien JA & Berger AJ (1999). Cotransmission of GABA and glycine to brain stem motoneurons. *J Neurophysiol* **82**, 1638–1641.

Okada M, Onodera K, Van Renterghem C, Sieghart W & Takahashi T (2000). Functional correlation of $GABA_A$ receptor α subunits expression with the properties of IPSCs in the developing thalamus. *J Neurosci* **20**, 2202–2208.

Pan Z-H & Lipton SA (1995). Multiple GABA receptor subtypes mediate inhibition of calcium influx at rat retinal bipolar cell terminals. *J Neurosci* **15**, 2668–2679.

Protti DA, Flores-Herr N, Li W, Massey SC & Wassle H (2005). Light signaling in scotopic conditions in the rabbit, mouse and rat retina: a physiological and anatomical study. *J Neurophysiol* **93**, 3479–3488.

Roska B, Nemeth E & Werblin FS (1998). Response to change is facilitated by a three-neuron disinhibitory pathway in the tiger salamander retina. *J Neurosci* **18**, 3451–3459.

Sagdullaev BT, McCall MA & Lukasiewicz PD (2006). Presynaptic inhibition modulates spillover, creating distinct dynamic response ranges of sensory output. *Neuron* **50**, 923–935.

Schnapf JL & Copenhagen DR (1982). Differences in the kinetics of rod and cone synaptic transmission. *Nature* **296**, 862–864.

Shields CR, Tran MN, Wong RO & Lukasiewicz PD (2000). Distinct ionotropic GABA receptors mediate presynaptic and postsynaptic inhibition in retinal bipolar cells. *J Neurosci* **20**, 2673–2682.

Slaughter MM & Miller RF (1981). 2-Amino-4-phosphonobutyric acid: a new pharmacological tool for retina research. *Science* **211**, 182–185.

Slaughter MM & Miller RF (1983). An excitatory amino acid antagonist blocks cone input to sign-conserving second-order retinal neurons. *Science* **219**, 1230–1232.

Strettoi E, Dacheux RF & Raviola E (1990). Synaptic connections of rod bipolar cells in the inner plexiform layer of the rabbit retina. *J Comp Neurol* **295**, 449–466.

Takahashi T (2005). Postsynaptic receptor mechanisms underlying developmental speeding of synaptic transmission. *Neurosci Res* **53**, 229–240.

Trexler EB, Li W & Massey SC (2005). Simultaneous contribution of two rod pathways to AII amacrine and cone bipolar cell light responses. *J Neurophysiol* **93**, 1476–1485.

Zhang J, Chang-Sub J & Slaughter MM (1997). Serial inhibitory synapses in retina. *Vis Neurosci* **14**, 553–563.

Acknowledgements

This work was supported by NIH grants T32 EY13360 and F32 EY15629 (E.D.E.); EY014701 (M.A.Mc.); EY08922 (P.D.L.), The M. Bauer Foundation (P.D.L.); EY02687 (Washington University, Department Ophthalmology) and Research to Prevent Blindness (Washington University and University of Louisville, Departments of Ophthalmology). We thank members of the Lukasiewicz and McCall laboratories and Dr Rachel Wong, for helpful discussion and comments on this manuscript and James Debrecht for technical assistance.